$Mo_6S_3I_6$ Nanowire Network Vapor Pressure Chemisensors

Miha Devetak, Bostjan Berčič, Marko Uplaznik, Ales Mrzel, and Dragan Mihailovic*

Jozef Stefan Institute, Jamova 39, SI-1000 Ljubljana, Slovenia, and Mo6 doo Teslova 30, SI-1000 Ljubljana, Slovenia

Received July 31, 2007. Revised Manuscript Received December 11, 2007

$Mo_6S_3I_6$ nanowire networks of interest are found to change their resistance in response to the presence of analyte vapors. The vapor sensing behavior is quantitatively described very well phenomenologically in terms of the concentration of adsorbed analyte molecules in the contact tunneling junctions, and an expression is derived for the dynamics and sensor resistance in terms of analyte vapor pressure. The time response of the sensor is observed to follow simple adsorption–desorption kinetics. The network sensor shows very clear selectivity, whereby the response is related to the dipole moment of the analyte. The response function favors rapid detection of small analyte concentrations.

Introduction

In recent years there has been a great deal of interest in new miniature nanowire and nanotube molecular sensors for rapid sensing of gases and vapors. The high surface-to-volume ratios associated with these nanostructures make their electrical properties extremely sensitive to species adsorbed on their surfaces and in the contacts between nanowires. The actual sensing mechnisms may be very different, however. Penner and co-workers[1] fabricated a hydrogen sensor using Pd nanowires supported on the surface of a polymeric thin film. Each nanowire contained many break junctions along their length. The gap between them changed as hydrogen gas was adsorbed into the Pd crystal lattice and the resistance of these nanowires exhibited a strong dependence on the gas concentration. In other experiments Cui and co-workers have modified the surfaces of semiconductor nanowires and implemented them as highly sensitive, real-time sensors for pH and biological species.[2] The mechanism was described in terms of the change in surface charge caused by protonation and deprotonation. More recently Law and co-workers fabricated a room-temperature photochemical NO_2 sensor based on individual single crystalline oxide nanowires and nanoribons,[3] where nitrogen dioxide acts as an electron-trapping adsorbate on SnO_2 surfaces and can be monitored by measuring the electrical conductance of the material.

To achieve recognitive detection of gases and vapors one needs to construct an array of different sensors, which have different responses to different analytes, so it is important to investigate new types of sensor materials. Li and co-workers[4] have demonstrated that chemisorbed species can also be detected as changes in conductance on gold metal nanowires. Early work on single wall carbon nanotubes (SWCNTs) has shown the conductance changes in response to the presence of molecular adsorbates on the surface of SWCNTs.[5] Different detection schemes have been used, such as detection of resistance,[6] field-effect transistor configurations,[7] and capacitance.[8] Snow and Perkins[6] have combined measurements of conductance and capacitance to extract intrinsic properties of the adsorbed species. Detailed vapor sensor measurements were reported recently on $Li_2Mo_6Se_6$ nanowire films.[9] There the resistivity was found to increase upon exposure to different analytes such as hexane, tetrahydrofuran, ethanol, and dimethylsulfoxide. The authors concluded that the resistivity increase is due to the change in interbundle contacts caused by the condensation of analyte molecules between the bundles, effectively reducing the hopping (tunneling) between individual bundles. Unfortunately, $Li_2Mo_6Se_6$ is sensitive to oxygen, which limits its usefulness as a practical sensor. In this work we report on the sensor properties of $Mo_6S_3I_6$, (MoSI) which is a new molecular nanowire material,[10] with electronic properties similar[11] to those of $Li_2Mo_6Se_6$, but is stable in air up to 200 °C and is chemically inert. MoSI molecular nanowires have rather unique functional properties, and they can be

(1) Walter, E. C.; Faview, F.; Penner, R. M. *Anal. Chem.* **2002**, *74*, 1546. Favier, F.; Walter, E. C.; Zach, M. P.; Benter, T.; Penner, R. M. *Science* **2001**, *293*, 2227.
(2) Cui, Y.; Wei, Q.; Park, H.; Lieber, C. M. *Science* **2001**, *293*, 1289.
(3) Law, M.; King, H.; Kim, F.; Messer, B.; Yang, P. *Angew. Chem., Int. Ed.* **2002**, *41*, 2405.
(4) Li, C. Z.; et al. *Appl. Phys. Lett.* **2000**, *76*, 1333.
(5) Kong, J.; et al. *Science* **2000**, *87*, 622. Collins, P. G.; et al. *Science* **2000**, *287*, 1801. Bekyarova, E.; Davis, M.; Burch, T.; Itkis, M. E.; Zhao, B.; Sunshine, S.; Haddon, R. C. *J. Phys. Chem. B* **2004**, *108*, 19717. Someya, T.; Small, J.; Kim, P.; Nuckolls, C.; Yardley, J. T. *Nano Lett.* **2003**, *3*, 877. Li, J.; Lu, Y.; Ye, Q.; Cinke, M.; Han, J.; Meyyappan, M. *Nano Lett.* **2003**, *3*, 929. Snow, S.; Perkins, F. K.; Houser, E. H. *Science* **2005**, *307*, 1942.
(6) Snow, E. S.; Perkins, F. K. *Nano Lett.* **2005**, *5*, 2414. Lonergan, M. C.; Severin, E. J.; Doleman, B. J.; Beaber, S. A.; Grubbs, R. H.; Lewis, N. S. *Chem. Mater.* **1996**, *8*, 2298. Favier, F.; et al. *Science* **2001**, *293*, 2227. Huang, X.; et al. *Nanotechnology* **2004**, *15*, 1284. Kim, Y. S.; et al. *Sens. Actuators, B* **2005**, *108*, 285.
(7) Wang, W. U. *Proc. Natl. Acad. Sci. U.S.A.* **2005**, *102*, 3208. Star, A.; Gabriel, J.-C. P.; Bradley, K.; Gruner, G. *Nano Letters* **2003**, *3*, 459; *Nano Lett.* **2003**, *3*, 1421.
(8) Snow, E. S.; Perkins, F. K. *Nano Letters* **2005**, *5*, 2414.
(9) Qi, X.; Osterloh, F. E. *J. Am. Chem. Soc.* **2005**, *127*, 7666. Qi, X.; Osterloh, F. E.; Barriga, S. A.; Giacomo, J. A.; Chiang, S. *Anal.Chem.* **2006**, *78*, 1306.
(10) Vrbanic, D.; et al. *Nanotechnology* **2004**, *15*, 635.
(11) Meden, T.; et al. *Nanotechnology* **2005**, *16*, 1578. Vilfan, I.; Mihailovic, D. *Phys. Rev. B* **2006**, *74*, 235411.

10.1021/cm703074f CCC: $40.75
Published on Web 02/01/2008

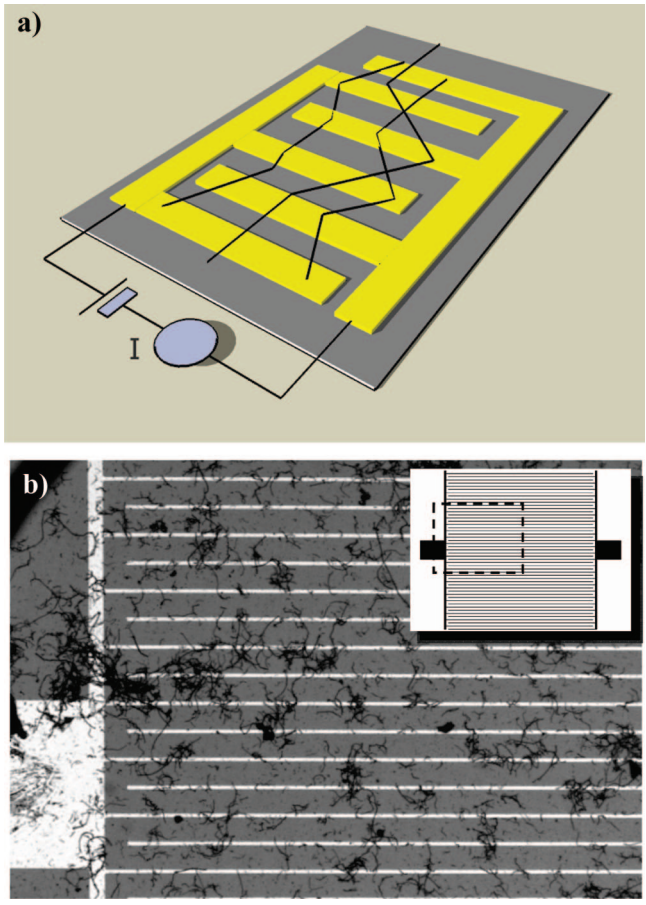

Figure 1. (a) Schematic diagram of the sensor circuit. (b) Scanning electron microscope image of a small section nanowire network circuit. The distance between fingers of the interdigital electrodes is 40 μm. The nanowires are randomly distibuted across the electrodes by placing a drop of nanowire solution in IPA and drying in air. The inset shows a schematic diagram of the entire circuit. The dashed square represents the image area.

easily synthesized[10] and dispersed in a variety of solvents[12] and are electrically conducting.[13] The electrical conductivity of MoSI networks (in pressed pellets) has been suggested to be largely determined by the junctions between wires,[14] suggesting its possible use in sensors. In this paper we present the first report of the material's sensing properties and show that the resistivity directly follows adsorption–desorption kinetics of analyte vapors. We also show that the sensing properties are not a result of the nanowires themselves, but rather their contact junctions. We investigate the response of networks of $Mo_6S_3I_6$ nanowires to a number of diverse analytes (methanol, ethanol, acetone, water, ammonia, chloroform, and pyridine) and show quantitative agreement with a theoretical model which we have developed to describe the observed behavior.

Experimental Setup

The measuring circuit consisted of Au-coated Ti interdigital electrodes 40 μm apart and 25 mm long, made with standard electron-beam lithography on an oxidized silicon wafer (Figure 1). The $Mo_6S_3I_6$ nanowires (supplied by Mo6 d.o.o.) were used as-produced, without any processing or purification. The nanowires were dispersed in isopropanol (IPA) solvent at a concentration of 0.1 mg/mL in an ultrasonic bath for 10 min and then deposited on the Ti/Au electrodes with a micropipette and dried. A section of the resulting circuit is shown in Figure 1b). Typically, sensor measurements are performed in vacuum, which makes the experiments easier and more controllable. In the case of $Li_2Mo_6Se_6$, the sensitivity to moisture prevents measurements in air. Here we have performed measurements in a flowing inert gas, which is much closer to a realistic sensing application and allows us to introduce high concentrations of analytes needed to test the model behavior also at high concentrations. The circuit was placed in a temperature-controlled sealed chamber and vapors at different concentrations are introduced into the sample space by mixing different proportions of pure (99.999%) nitrogen gas with the flow of saturated analyte vapor at 296 K. The saturated vapors were produced by bubbling nitrogen gas through analyte liquid at flow rates from 0.05 to 0.8 L/min. The temperature was kept constant at 296 K for all the measurements. The total flow rate was kept constant (10 L/min); only the ratio between saturated vapors and pure nitrogen was varied. The resolution of the concentration (particularly at low flow rates) is limited by the accuracy of the flow control valves (Cole-Parmer EW-98450-33). Before each measurement, the sensors were purged with a steady flow of nitrogen gas. Three circuits made this way showed very similar response, the average deviation between points being less than 17%, showing that the circuit easily is quantitatively reproducible and that there are no uncontrolled impurities in the junctions which might influence the response. The ratio between flow of saturated vapor and the total flow $f = F_S/F_T$ was varied from 0.5 to 8%. The resistance of the nanowire network was monitored with a Keithley 2000 multimeter.

Experimental Results

The typical change of resistance upon exposure to methanol vapor is shown in Figure 2a. In all the analytes which we have tested, the resistance *increases* upon exposure to the vapor.

In Figure 2b we see that the response upon switching off the analyte flow is the same for all concentrations, while the "on" response is faster for larger analyte concentrations. The response to ethanol, water, acetone, ammonia, and chloroform is very similar to the one shown in Figure 2a. The time response appears to be determined by the adsorption/desorption dynamics and not by the gas flow. The response is nearly exponential, which we will discuss later, and appears to be intrinsic. The change of resistance is shown quantitatively in Figure 3a, where we plot the normalized change of resistance $\Delta R/R$ versus partial pressure of the analyte P_A. Here R is the total circuit resistance and the concentration is expressed in terms of ppm. The behavior of all analytes is qualitatively very similar, all showing a clearly resolved rapid initial increase of $\Delta R/R$ at the lowest concentration (0.5%) and then a gradual saturation at higher P_A.

Next, we investigate whether the change in overall resistance is due to the response of the individual bundles themselves and the contacts between two of them. To test whether R_{NW} changes upon exposure to the analytes, we first made a test circuit using a single 1 μm diameter nanowire bundle stretched between two silver paste contacts 100 μm apart. The nanowire showed no detectable change of R_{NW}

(12) McCarthy, D. N.; et al. *J. Appl. Phys.* **2007**, *101*, 014317.
(13) Uplaznik, M.; et al. *Nanotechnology* **2006**, *17*, 5142. Kutnjak, Z.; et al. *J. Appl. Phys.* **2006**, *99*, 064311.
(14) Berèiè, B. *Appl. Phys. Lett.* **2006**, *88*, 173103.

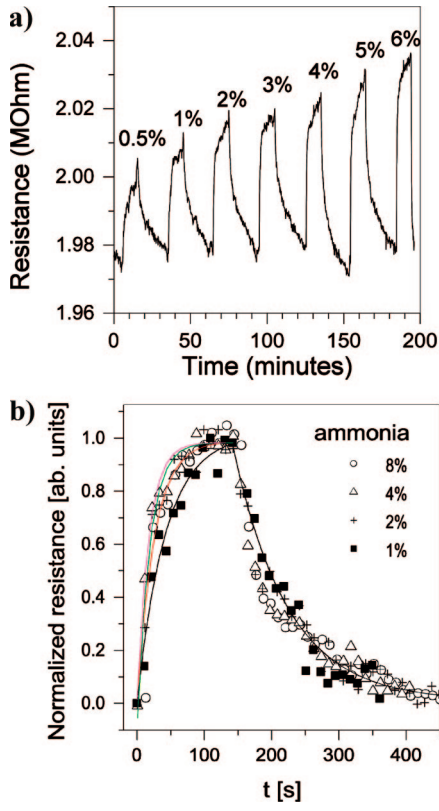

Figure 2. (a) Resistance of the MoSI network circuit after exposure to different concentrations of methanol vapor, measured as a percentage of saturated vapor pressure at 296 K. (b) Sensor (shown here for ammonia) gives a noticeably faster rise time than fall time. The risetime appears to decrease on increasing analyte concentration. The solid lines are exponential fits to the data (see text).

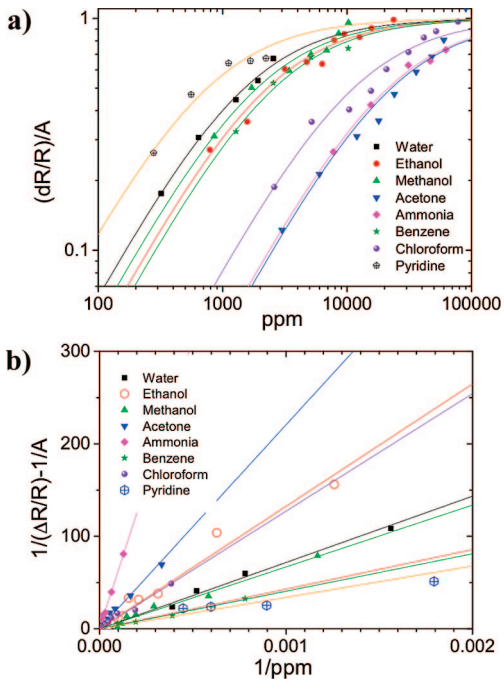

Figure 3. (a) Normalized change in resistance $\Delta R/R \times A$ versus analyte partial pressure P_A (expressed as concentration C in ppm) for methanol, ethanol, acetone, chloroform, water, pyridine, and ammonia. The solid lines are fits to the data using eq 3 (see text). (b) A plot of $1/(\Delta R/R) - 1/A$ vs $1/P_A$ (again in terms of concentration in ppm), where the intercept $1/A$ is subtracted and is plotted in Figure 4b. The slope of the straight line gives Ak_BT/K, from which we can calculate K in eq 3 (see text).

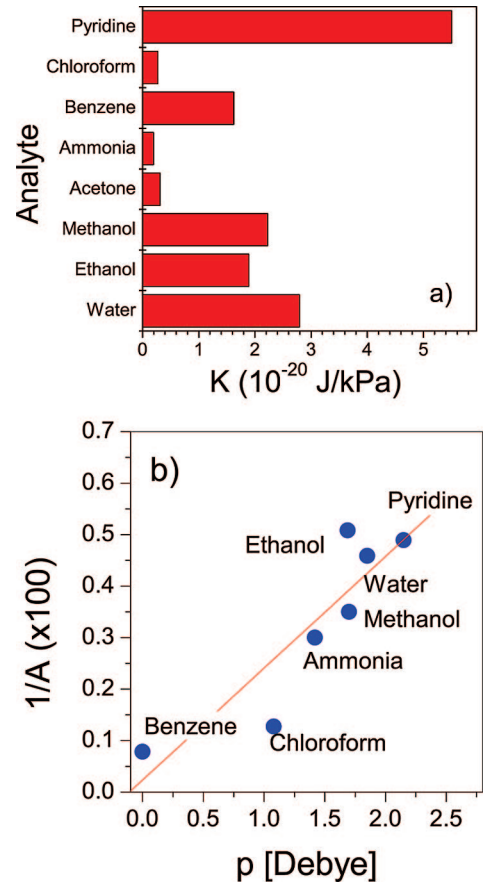

Figure 4. (a) Constant K at 20 °C for different analytes. (b) Response constant $1/A$ vs dipole moment of the analyte.

upon exposure to an accuracy of $\Delta R/R < 3 \times 10^{-4}$. Next we prepared a similar circuit but with two crossed nanowires in contact, testing the resistance of both the individual nanowire bundles and the contact junction formed by two touching nanowires. Surprisingly, we found that the junction contact resistance did not change upon exposure to analyte, to the same accuracy of $\Delta R/R < 3 \times 10^{-4}$. The two observations strongly suggest that the main sensing properties of the present circuit arise from the change of resistance at the bundle−metal contacts. This is also confirmed by the fact that different contact metal electrodes give qualitatively different responses. We will discuss this point again below when we discuss the model predictions for nanowire networks.

Discussion

Having determined that individual nanowires are not sensitive to the presence of the analyte, the main effect which is relevant to describing the sensor properties is the condensation of analyte molecules in the network contacts with the metal. To describe the effect, we first calculate the equilibrium number of molecules in the junctions. Let us suppose that there are a limited number of molecules that can fit in the junctions, N_0, and that a fraction ν of this number is present at any given temperature T and analyte pressure P_A. The analyte desorption rate is then given by $k_D \nu N_0$, where k_D is an analyte-specific desorption rate. Similarly, the rate of adsorption of molecules in the junction can be written as

$k_A(1 - \nu)N_0n$, where n is the number of analyte molecules per unit volume in the surroundings and k_A is the adsorption rate. The dynamics of analyte molecule concentration in the junction at any given time is then governed by

$$\frac{d\nu}{dt} = -k_D\nu N_0 + k_A(1 - \nu)N_0n \quad (1)$$

The solution to eq 1 is given by

$$\nu = b/(a + b) + \exp[C(a + b) - t(a + b)] \quad (2)$$

where $a = k_DN_0$, $b = k_DN_0n$, and C is a constant. Upon switching *off* the analyte flow ($b = 0$), the solution (eq 2) is a simple exponential, $\nu = \alpha \exp[-ta]$. Upon switching *on* the analyte, the response (eq 2) is still exponential but depends on analyte concentration n.

Assuming for the moment that the measured response $\Delta R/R$ is proportional to ν, we can see that just such behavior is observed in our measurements, as shown in Figure 2b: the "*on*" response time shortens with increasing n, while the "*off*" response is slower and appears to be independent of n, as predicted by eq 2.

In equilibrium (i.e., after the system has equilibrated), the adsorption and desorption rates are equal, so eq 1reduces to $k_A(1 - \nu)N_0n = k_D\nu N_0$. The equilibrium occupancy of molecules in the junction ν is then given by $\nu = Kn/(1 + Kn)$, where $K = k_A/k_D$. Or, expressing ν in terms of analyte partial pressure P_A, for low pressures we can write $P_A = nkT$, so $(1/\nu) = 1 + (1/BP_A)$ where $B = K/k_BT$.[15] Note that adsorption and desorption in the junction are governed by thermally activated processes, so K is also expected to be temperature dependent, $K = K_0 \exp[(E_A - E_D)/kT]$, where K_0 is a constant and E_A and E_D are the adsorption and desorption energy barriers, respectively.

Assuming that the additional junction resistance due to the presence of the analyte is directly releated to the decrease in tunneling probability in the junction, which is in turn related to the number of molecules present in the junction ν, then $\Delta R = A\nu$ describes the dependence of the circuit resistance on the relative vapor pressure P_A, where A is some function of T and ν, describing the resistive response of the junction network. To first approximation let us assume here that A is a constant at constant temperature. The result is a relation:

$$\frac{1}{\Delta R/R} = \frac{1}{A}\left(1 + \frac{k_BT}{KP_A}\right) \quad (3)$$

which is plotted in the form of fits to the data in Figure 3a for a number of analytes. Plotting $1/(\Delta R/R)$ versus $1/P_A$ (expressed in ppm) in Figure 3b, the intercept gives $1/A$, and the slope is Ak_BT/K, from which we can calculate K. We see in Figure 3 that despite the relatively crude measurement technique ΔR closely follows the predicted behavior given by eq 3. The values of K and A obtained in this way are shown in Figure 4a for different analytes. Finally, in Figure 4b we show $1/A$ versus dipole moment p of the analyte. Empirically, a clear correlation between $1/A$ and p is evident.

(15) Note that the steady state solution is formally identical to the Langmuir equation describing the adsorption of molecules confined by a potential energy minimum on the surface. Langmuir, I. *J. Am. Chem. Soc.* **1916**, *38*, 2221.

Turning to the question of why the resistance increases in the presence of the analyte, we can first try and analyze the conductance of the network using the variable range hopping (VRH) model in the coulomb regime[16] adapted for the case of a nanowire network by Hu and Shklovskii[17] which was recently applied to the case of carbon nanotubes dispersed in a polymer host matrix.[18] The effect of increasing inter-bundle spacing (swelling) due to the introduction of analyte in our circuit may be thought of as playing a role similar to that of changing the dilution in the case of the CNT/polymer composites. At relatively low density $1/dL^2 > n > 1/L^3$ where L is the average bundle length, d the average diameter, and n is their number density, the conductivity is given by $R = R_0 \exp(T_0/T)^{1/2}$, where, in the Efros−Schkolvskii model, $T_0 = e^2/[\epsilon\epsilon_0 a(nL^3)^2]$. Here a is the tunneling distance through the analyte in the junction and ϵ is the dielectric constant of the medium in the junction. We see that the predicted resisitivity in the ES model is exponentially dependent on the dielectric constant in the junction and its thickness. Because the condensation of analyte into the junction is expected to increase the conductivity σ (replacing nitrogen by the analyte in the junction) and probably also increase a, both would have the effect of decreasing T_0, which should *decrease* R, not increase it. A similar drop in R is also expected for the Mott VRH model where $T_0 = 1/(N(0)\xi^3)$, where $N(0)$ is the density of states in the nanowire and ξ is the localization length (which can be related to the inter-bundle distance a, similar as in the ES model). Clearly increasing ξ has the same effect as decreasing R in the Mott VRH model as well. It appears that neither the ES nor Mott VRH models can be directly applied to the observed sensing behavior of the MoSI internanowire tunneling, and the dominant effect of increased resistance is thus suggested to be a consequence of the reduced tunneling rate in the metal−nanowire contact junctions, as suggested by the two-crossed-nanowire experiment. To first approximation, we see that the linear relation between the analyte concentration in the junctions and the excess resistance ΔR gives good agreement with the data (Figure 3a,b).

We see from Figure 3 that, for small concentrations, the predicted response of the sensor is very large and linear. However, in this work we were mainly interested in determining the intrinsic sensing mechanism, and no attempt was yet made to test or optimize the sensitivity at low concentrations. Importantly, we see that the absolute change of resistance of the junctions on exposure to the analyte is large (on the order of 10–100 kΩ), which translates into a potentially large sensitivity. Reducing the circuit overall impedance would drastically improve the sensitivity and increase $\Delta R/R$. The major part of the circuit resistance R comes from the longitudinal resistance R_{NW} of the nanowires themselves, and it would be useful if this could be reduced. Postprocessing procedures of MoSI nanowire material have

(16) Efros, A. I.; Shklovskii, B. I. *J. Phys. C: Solid State Phys.* **1975**, *8*, L49.

(17) Hu, T.; Shklovskii, B. I. *Phys. Rev. B* **2006**, *74*, 174201; *Phys. Rev. B***2006**, *74*, 054205; *Phys. Rev. B***2006**, *73*, 155434. Mott, N. F.; Davis, E. A. *Electronic Processes in Non-Crystalline Materials*; Clarendon: Oxford, 1979.

(18) Benoit, J. M.; Corraze, B.; Chauvet, O. *Phys. Rev. B* **2002**, *65*, 241405.

recently been discovered to reduce the resistivity R by more than 5 orders of magnitude,[19] which would translate into a large increase in sensitivity. Further, the circuit shown in Figure 1 is very sparse in terms of junctions. Optimization of the junction density and interelectrode distance would strongly boost the sensitivity further.

In conclusion, we note that the main advantages of MoSI nanowires as a sensor over existing vapor pressure sensors are its simple resistive response, chemical stability, ease of construction, and potentially high sensitivity. The theoretical model which we have developed gives a quantitative description of the sensing time dynamics, temperature dependence and response in terms of analyte concentration in the sensor contact junctions over a wide range of concentrations. After optimization of the intrinsic material resistance, network electrodes, and nanowire density to reduce the overall resistance and reduce external noise, the sensor promises to be a practically useful device, whose response function (Figure 3 and eq 3) makes it useful for the detection of different analytes over a very large range of vapor pressures.

Acknowledgment. We wish to thank Boris I. Shklovskii, Tomaz Mertelj, and Viktor Kabanov for useful discussions.

CM703074F

(19) Hummelgard, M.; et al., in preparation.